An Efficient Epilepsy Prediction Model on European Dataset with Model Evaluation Considering Seizure Types

Shiva Maleki Varnosfaderani, Ian McNulty, Nabil J. Sarhan, Waleed Abood, and Mohammad Alhawari

***Abstract*— This paper develops a computationally efficient model for automatic patient-specific seizure prediction using a two-layer LSTM from multichannel intracranial electroencephalogram time-series data. We decrease the number of parameters by employing a smaller input size and fewer electrodes, thereby making the model a viable option for wearable and implantable devices. We test the proposed prediction model on 26 patients from the European iEEG dataset, which is the largest epileptic seizure dataset. We also apply an automatic preprocessing technique based on a common average reference to remove artifacts from this dataset. The simulation results show that the model with its simple structure in conjunction with the mean post-processing procedure performed the best, with an average AUC of 0.885. This study is the first that utilizes the European database for epilepsy prediction application and the first that analyzes the effect of the seizure type on the system performance and demonstrates that the seizure type has a considerable impact.**

***Index Terms*— Deep learning, epileptic seizure prediction, European iEEG dataset, preprocessing, two-layer LSTM, seizure type.**

I. Introduction

EPILEPSY is a disease of the brain characterized by repeated seizures, at least two seizures, that are not brought on by other illnesses [1]. Although the exact cause is usually unknown, epileptic seizures can be caused by brain damage or a genetic susceptibility [2]. The United States accounts for 3.4 million of the world's epilepsy patients, according to the World Health Organization [3]. The International League Against Epilepsy (ILAE) has replaced "epilepsy disorder" with "epilepsy disease" to emphasize its gravity and impact. However, concerns persist about potential stigma. Individuals with epilepsy face a heightened risk of bodily harm, with Sudden Unexpected Death in Epilepsy (SUDEP) being the leading cause of mortality. Uncontrolled seizures also lead to difficulties in employment and driving, exacerbating socioeconomic challenges. Chronic uncontrolled epilepsy is linked to anxiety, suicidal ideation, and other psychiatric disorders, impacting both individuals and families [4].

Generally, epilepsy research can be divided into four main categories: (1) anti-epileptic medications, (2) epilepsy localization and surgery, (3) epilepsy detection, and (4) epilepsy prediction. Anti-epileptic medications are currently the basis of epilepsy therapy. Unfortunately, despite receiving therapy, over 30% of people with epilepsy continue to experience seizures [5]. The other 70% of patients who react to anti-epileptic drugs experience unfavorable side effects, such as nausea, fatigue, dizziness, or impaired vision. When drugs are unable to manage seizures, epilepsy surgery may be a possibility. This surgical technique involves resecting a portion of the brain that causes seizures, which helps to halt seizures or lessen their frequency. However, it might come with significant consequences, such as paralysis, stroke, vision damage, and memory and language issues [6], [7]. In epilepsy detection, on the other hand, the patients do not have enough time to react to the seizure. Therefore, there has been much interest in creating tools for seizure forecasting. Epileptic seizure prediction has the potential to significantly improve patient care by warning them of imminent seizures and allowing them to prepare a quick-acting drug and take steps to prevent any potential harm. It also paves the way for customized medicines with fewer adverse effects for each individual with epilepsy, and thus seizure intervention systems may be utilized to prevent upcoming seizures [8].

Electroencephalography (EEG) is a key tool for identifying a variety of brain illnesses, including epilepsy [9]. *Preictal*, *ictal*, *postictal*, and *interictal* are the four basic states for EEG signals in epilepsy, which relate to the time before the onset of the seizure, the seizure onset time, the time after the seizure onset, and the time during normal brain activities, respectively [10]. EEG signals can be divided into two primary groups called *scalp EEG* (sEEG) and *intracranial EEG* (iEEG) based on where the electrodes are placed. sEEG does not require invasive operation and can be captured by placing the electrodes on the scalp. In contrast, implant surgery is needed to record the iEEG data, which is mostly utilized to record

Shiva Maleki Varnosfaderani is with the Electrical Engineering Department, Wayne State University, Detroit, MI, USA (e-mail: shiva.maleki.varnosfaderani@wayne.edu).

I. McNulty is with the Computer Science Department, Wayne State University, MI, USA (e-mail: gi5631@wayne.edu).

N. J. Sarhan, is with the Faculty of Computer Engineering Department, Wayne State University, MI, USA (e-mail: nabil.sarhan@wayne.edu).

Waleed Abood is with the Faculty of Neurology, Wayne State University School of Medicine, MI, USA (e-mail: wabood@med.wayne.edu).

M. Alhawari is with the Faculty of Electrical Engineering Department, Wayne State University, MI, USA (e-mail: alhawari@wayne.edu).

Manuscript received; revised. Corresponding author: Mohammad Alhawari

long-term EEG data [11].

EEG signals can be compromised by both internal and external abnormalities, leading to a deterioration in signal quality [12], [13]. There are several denoising techniques reported in the literature to remove various noise types from EEG data [14]–[20]. Re-referencing techniques can eliminate common noise present in EEG electrodes caused by the movement of the reference electrode or the noise from the data-gathering instruments connected to the electrodes. Bipolar, Laplacian, and average re-referencing techniques, among others, can be employed to reduce the impact of common noise. Stereo EEG electrodes can be utilized with either the bipolar or average Laplacian methodology, while subdural electrodes are frequently employed with the average Laplacian technique [21]–[23].

This paper develops and validates an epileptic seizure prediction system employing a two-layer Long Short-Term Memory (LSTM) model that is capable of predicting seizures reliably and accurately using four EEG channels. The system is validated on the European database, the largest EEG dataset, marking the first instance of its application in epilepsy prediction. The primary contributions of this paper are outlined as follows:

- introducing a denoising-preprocessing approach utilizing the Common Average Reference (CAR) method for cleaning raw iEEG data,
- introducing handcrafted time and frequency domain EEG features optimized for epilepsy prediction,
- proposing an efficient LSTM model that utilizes only four channels per patient, leading to a substantial reduction in system complexity,
- assessing the system performance using the European iEEG dataset,
- evaluating the system performance across a significant number of patients (26 patients),
- using the origin electrodes for the simulations, and
- interpreting the results based on seizure types.

To the best of our knowledge, this is the first study making a connection between model performance and seizure types which may help doctors better diagnosing epileptic patients.

The rest of this study is organized as follows. A literature review is performed in Section II. Section III describes the EEG dataset used to evaluate the proposed system. Section IV presents the proposed epilepsy prediction model based on a two-layer LSTM. Discussion and future work are introduced in Section V. Finally, the conclusions are drawn.

II. Prior Work on Epilepsy Prediction Systems

Recent advancements in Deep Learning (DL) techniques have led to the development of highly accurate epilepsy prediction systems [24]–[34]. To construct an intelligent epilepsy prediction system based on DL, various procedures such as *preprocessing*, *feature extraction*, *classification*, and *post-processing* are essential. Preprocessing uses filtering, artifact removal techniques, and augmentation to prepare and remove noise from EEG data. In contrast to processing raw EEG signals, the complexity and computational cost of the system are reduced by employing channel-based and segment-based feature extraction [35]. Channel-based feature extraction refers to features extracted from each EEG channel, including statistical time-domain features (such as mean, variance, kurtosis, and skewness), frequency-domain features (such as spectral power in various frequency bands and *Short-Time Fourier Transform (STFT)*), and wavelet-domain features. Systems can have shorter training durations, less complexity, and lower power consumption when handcrafted features are used, compared to systems that automatically extract features using Convolutional Neural Networks (CNNs). In [36], *Common Spatial Pattern* (CSP) is used to extract 324 (18×18) features from 23,040 data points to decrease the number of trainable parameters using CNN, however, the model suffer from low sensitivity. CNN [25], [29]–[31], [33], [37]–[39], LSTM [26], [40], *Bidirectional LSTM* (BiLSTM) [24], [41], and *Convolutional Gated Recurrent Neural Network* (CGRNN) [28] are examples of classifiers that are used to categorize EEG data. The *K-of-N* [25], mean, and minimum distance (MD) [34] approaches have been utilized as post-processing techniques to improve classification accuracy while lowering the false prediction rate (FPR).

A CNN with six convolutional layers and two fully linked layers is developed in [30]. The model is evaluated on two separate sEEG datasets, including a subset of the public CHB-MIT EEG database and the dataset collected at the Mount Sinai Hospital. The CNN obtained a prediction sensitivity of 87.8% and FPR of 0.142/hr when trained on 3D wavelet tensors generated from the wavelet transformation of raw sEEG data. Similar study can also be found in [42], where STFT is used to convert raw EEG signals into time-frequency characteristics. The resulting image-like 2D features are then fed into a CNN that includes three convolution blocks and two fully linked layers. When evaluated on datasets from Freiburg Hospital, CHB-MIT, and the American Epilepsy Society (AES) Seizure Prediction dataset, the suggested model has a sensitivity of 81.4%, 81.2%, and 75%, respectively. In [43], a CNN model is trained on channel-frequency feature maps, generated by the directed transfer function (DFT), achieving a sensitivity of 90.8% and an FPR of 0.08/h are obtained using Freiburg EEG dataset.

Most of the reported epileptic systems achieved good model performance, however, their high computational resource and memory bandwidth demands restrict their implementation in resource-constrained devices such as wearable and implantable devices. [44] proposed a power management model based on patient-specific seizure patterns to control the overall system's power consumption. This model identifies the patient-specific seizure pattern and transitions the system into sleep mode during periods when the likelihood of a seizure is negligible or extremely low. The suggested power management model has the potential to significantly decrease power consumption by 49% compared to a more complex model, with a minimal performance reduction of less than 1%. Recently, LSTMs have been applied in applications for epilepsy prediction due to their capacity for learning long-term dependencies [24], [26], [27], [34]. In [26], LSTM is used to analyze the EEG signals for epileptic seizure prediction, where 643 features in time and

This article has been accepted for publication in IEEE Journal of Biomedical and Health Informatics. This is the author's version which has not been fully edited and content may change prior to final publication. Citation information: DOI 10.1109/JBHI.2024.3423766

frequency domains are selected from each 5-second segment and sent into a two-layer LSTM with 128 memory units in each layer, creating a huge model with more than 500,000 trainable parameters. In [24], 10 channels that obtain the same level of prediction accuracy are chosen based on the highest variance entropy product. The used channel selection method eliminates redundant and unnecessary channels which brings the total number of trainable parameters down to 18,345 for a Deep Convolutional Autoencoder (DCAE) + BiLSTM model. Although the suggested structure achieves high sensitivity and low FPR, the system's effectiveness is assessed by a small number of patients from CHB-MIT database [45], [46]. In [34], a model with two-layer LSTM showed a good performance with AUC score of 0.920, verified on the Melbourne dataset. The study uses handcrafted features from the EEG signals, including temporal data (such as mean, variance, and peak-to-peak values) and spectral information (such as spectral power in eight canonical EEG frequency bands), fed into LSTM network. In [47], another LSTM-based seizure prediction technique uses statistical information extracted from EEG rhythms as inputs. When evaluated on the Melbourne dataset, it achieved an AUC score of 0.894.

The imbalanced data problem affects epilepsy prediction systems since there are more interictal samples than preictal samples, thereby resulting in a biased model in favor of interictal samples [48]. A number of methods, such as *Overlapping Sampling* [25], *Generative Adversarial Network* (GAN) [29], and *Deep Convolutional Generative Adversarial Networks* (DCGAN) [32] can be used to produce synthetic EEG data to overcome this issue.

III. European iEEG Dataset and Its Challenges

The European iEEG Epilepsy dataset is among the largest available datasets for epileptic seizure applications [49]. The dataset provides comprehensive details of each patient, including age, gender, disease history, surgical process and outcomes, the onset zone of seizures, and electrode type and placement. For each patient, the EEG onset and clinical onset are reported. EEG onset is generally assigned several seconds to several minutes earlier than the clinical onset (which is related to the first clinical signs). Each interictal file consists of a one-hour recording with a two-hour gap before and after EEG onset time to avoid overlapping. In our study, the preictal samples are extracted one hour before seizure onset with a five-minute gap from the EEG onset to avoid overlapping. 26 patients from this dataset are used to evaluate the performance of the proposed system. More details about this dataset can be found in [20] and [50].

A. Challenges in the European iEEG Dataset

In our study, as presented in [20], we utilized the European dataset for the first time to assess the effectiveness of a common average reference technique to mitigate the noise introduced by the common scalp reference. We encountered several challenges, including identifying and removing dropout channels and segments, reducing the noise caused by the scalp reference used for data recording, managing large noise spikes

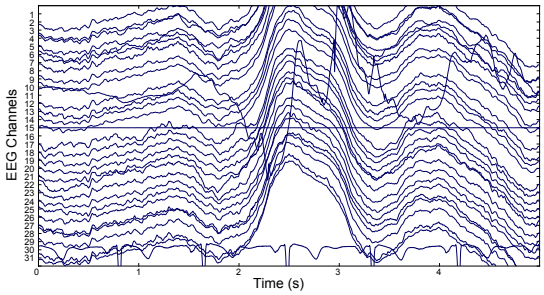

Fig. 1. An example of common noise in iEEG dataset [20].

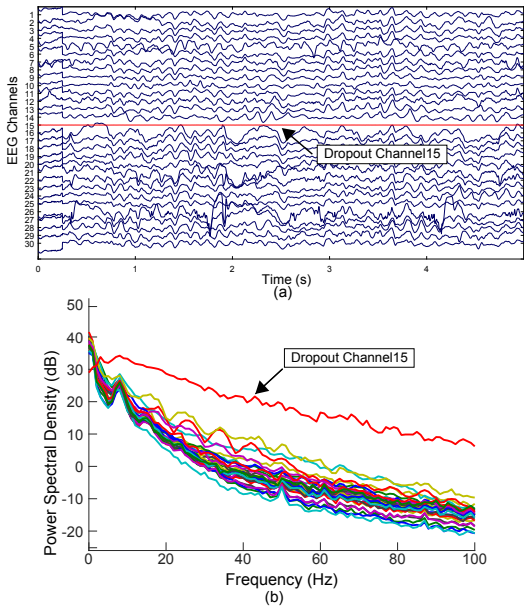

Fig. 2. The representation of Dropout channels in time and frequency domain. a) Time domain representation where the red channel consists of dropout data. b) Frequency domain representation where the red channel consists of drop out channel [20].

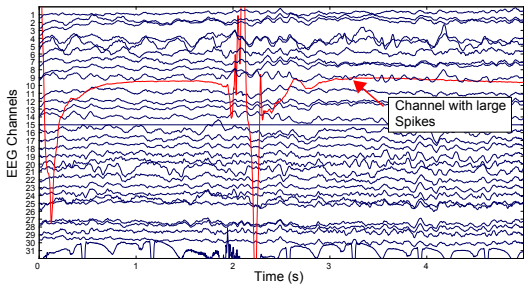

Fig. 3. An example of an electrode with a large spike, which is not due to common noise [20].

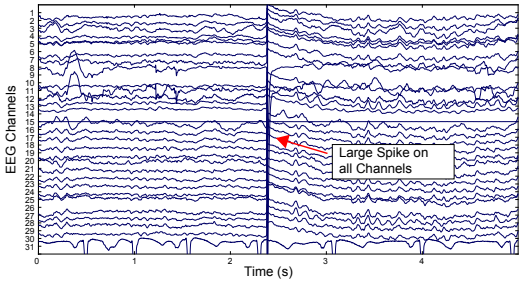

Fig. 4. Large spikes appear in all EEG channels [20].

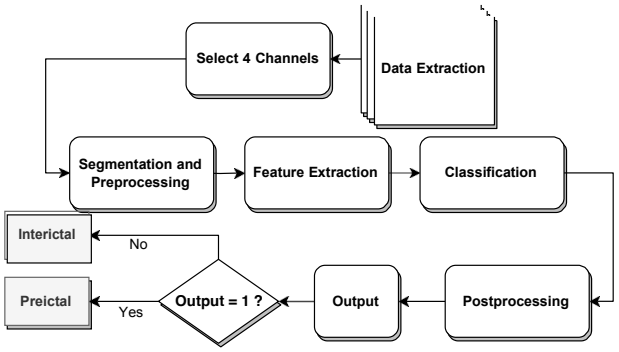

Fig. 5. Proposed epilepsy prediction system for the European Dataset.

that are possibly induced by electrode disconnection, and recording subclinical seizures. The dataset consists entirely of raw data without any preprocessing, posing difficulties in cleaning the data from various types of noise. Although the dataset includes iEEG data, which is less susceptible to noise, a scalp EEG electrode serves as a reference electrode. Therefore, the noise generated from the scalp electrode manifests in the iEEG data as common noise.

Figures 1-4 present some of types of noise exist in the European dataset. Figure 1 shows an example demonstrating the influence of common noise on EEG channels in time domain, caused by the movement of the reference electrode, motion artifacts, such as muscle movements, and eye blinking. Figure 2 illustrates the difference between the dropout channel (channel 15) and other channels in time and frequency domain. Several files in this dataset have multiple electrodes with low or constant values, which do not represent EEG data and thus can be considered as dropout data. Based on their power level, the dropout channels may be quickly identified in the frequency domain. Figure 3 displays a large spike in one channel, represented by red color, which can be due to disconnection of the scalp electrode. Figure 4 displays large spike in one channel causing a large amplitude on all of the channels, which can be due to common noise.

IV. Proposed Epilepsy Prediction Machine Learning Model

The proposed epilepsy prediction system, designed for the European dataset, is illustrated in Figure 5. As shown in the figure, the details of the model are described as follows.

1- **Data Extraction**: A one-hour EEG data with 5 minutes gap from the EEG onset is considered to extract preictal samples to avoid overlapping with the ictal state. Every interictal file lasts for one hour, where we consider the two-hour intervals before and after the EEG onset time to extract the interictal files.

2- **Channels Selection**: We select four EEG channels based on the following criteria: 1) proximity to the brain's lobe area where seizures start, 2) coverage of a large brain area, 3) inclusion of at least two seizure onset zone electrodes, and 4) exclusion of dropout electrodes. Furthermore, we assume that experts accurately assigned the origin electrode, as included in the dataset. More details can be found in our previous research [20].

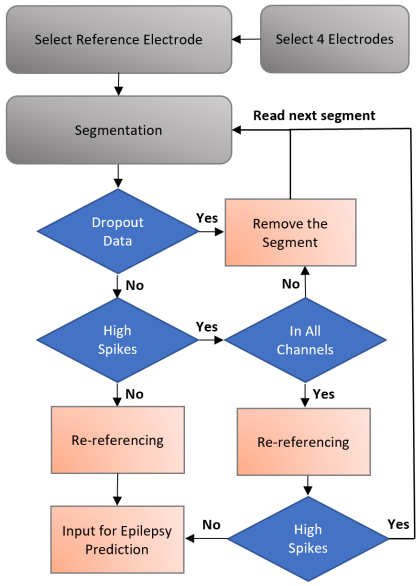

Fig. 6. The proposed preprocessing method based on the re-referencing method in [20].

3- **Segmentation and Preprocessing**: Each 60-minute raw iEEG clip is divided into 5-second non-overlapping segments, and every 6 consecutive segments are grouped together as an LSTM input. Each preictal group is assigned a label of one, and each interictal group is assigned a label of zero. After that, the preprocessing is applied to clean each segment based on CAR method, as shown in Figure 6 [20]. As depicted in the figure, once the four electrodes are selected, the segments are cleaned based on the following steps. 1) The power line noise is eliminated using a notch filter set to a 50 Hz frequency. 2) If the algorithm finds a dropout data (more than 20% of the segment), then the segment is discarded and the following segment is processed. 3) The system detects large spikes in the data when the peak-to-peak value surpasses a specific threshold. If a large spike is present in all channels, it is considered common noise, which is then removed using the re-referencing method described in [20]. In contrast, if a large spike is observed in one, two, or three electrodes, then these electrodes are likely disconnected and the segment is discarded. Note that the threshold for identifying large spikes is set to 5000 μV for this dataset.

4- **Feature Extraction**: Six features in time domain and seven features infrequency domain are extracted for each channel. The time-domain features consist of energy distribution, deviation, peak-to-peak values, and the number of zero-crossings, as well as two statistical moments: *skewness* and *kurtosis*. The frequency-domain features include the spectral power intensity, which is extracted from the EEG data for 7 frequency bands from 0.1 Hz to 100 Hz using PyEEG library [51], including 0.1-4 Hz, 4-8 Hz, 8-12 Hz, 12-30 Hz, 30-50 Hz, 50-80 Hz, 80-100 Hz.

5- **Classification**: A two-layer LSTM is used to classify the data into preictal and interictal classes. Five different LSTM sizes are used to investigate the effect of the model's size on the results. Model 1 is the simplest model which consists of

two layers with 16 memory units, while Model 5 consists of two layers with 256 memory units. The models are followed by a fully connected layer with an output of 30 to 100 units using the "ReLU" activation function and a final dense layer using "Sigmoid" activation function. The output is assigned to one for preictal samples and zero for interictal samples with a threshold of 0.5. More details about each model are shown in Figure 7. For all models, the Binary Cross-Entropy function is selected as the loss function, and the Adaptive Moment Estimation (Adam) with a learning rate of 0.001 is used as the optimizer. The Leave-one-out cross-validation (LOOCV) technique is utilized to evaluate the performance of the system. In the LOOCV technique, in each round, one preictal file and N interictal files (to cover almost all data for the test part which is dependent on the total number of interictal files) are separated for testing, and the rest of the samples are used for training. For instance, we may have 50 interictal samples and 5 preictal samples for a single subject. Thus, we perform five test and training rounds for this patient, where we exclude one preictal sample and ten interictal samples in each round. The Models are trained with an equal number of interictal and preictal samples from the training samples to address the unbalanced dataset issue. Dropout is applied to the first and second layers with a factor of 10% and 30%, respectively, to prevent overfitting. The number of epochs utilized for model training ranged from 100 to 500. In this case, the early stopping technique is implemented to stop the training before convergence to avoid the overfitting [52].

6- **Postprocessing**: Three post-processing methods are applied, including *arithmetic mean*, *k-of-n* [42], and minimum distance (*MD*) [34] to assign an output to ten sequence outputs from LSTM. In our study, we chose the values of k to be 5 and n to be 10. The MD method aims to determine the similarity between network outputs and either interictal or preictal samples. To make a decision about a sequence of outputs and assign a final output, the method assesses whether the output is closer to zero (representing interictal samples) or closer to one (representing preictal samples). In the following, more details about MD method are provided:

- Identify Extremes: Determine the minimum and maximum of the n-sequence output of the LSTM network.

- Calculate Distances: Calculate the distance between the minimum and zero (stored as dis-min) and the distance between the maximum and one (stored as dis-max). The objective of this step is to assess the similarity of the output to both interictal and preictal samples.

- Comparison: Compare dis-min and dis-max to decide the final output. If dis-max is lower than dis-min, indicating similarity to preictal samples, assign the output as one. Otherwise, assign it as zero, representing interictal samples.

Figure 8 illustrates an example of how the MD technique operates, where each point on the y-axis represents an LSTM output, while the x-axis shows the sequence of outputs. In the proposed system, the output is zero for interictal samples and one for preictal samples. Each set of five-sequence outputs of the LSTM (n=5) is condensed into one output during post-processing. In this example, the first and second sequence outputs are interictal samples. For both sequences, the dis-min values of 0.13 and 0.26 are lower than the dis-max values of 0.23 and 0.44, respectively. Therefore, the final output is correctly assigned to zero. However, for the first sequence output, the output is assigned to one using the mean and k-of-n method.

A. Evaluation of the Effect of Postprocessing on the Results

To assess the performance of the proposed model, simulation results for 26 patients from the iEEG European dataset are presented, utilizing metrics such as sensitivity, false prediction rate (FPR), accuracy, and area under the Receiver Operator Characteristic (ROC) curve (AUC). The results for each patient and the average results for each model are presented in Tables I-V for models 1-5, respectively. As shown in Tabel I, for all patients except Pat-970, Pat-958, Pat-620, Pat-635, Pat-264, Pat-583, Pat-548, Pat-115, and Pat-442, the mean method has the best AUC, and k-of-n has the worst AUC. In these patients, the MD has the best AUC compared to the mean and k-of-n methods. The average results indicate that the mean method in the post-processing presents the best AUC compared to MD and k-of-n. Pat-253 has the lowest AUC compared to other patients, where the data are from a 37-year-old woman whose epilepsy began when she was 18 years old.

Several hypotheses could explain the sub-optimal performance of the model. First, the data are recorded over 10 days, during which the patient underwent more than 70 subclinical seizures in a condensed time frame. Although the subclinical seizures are identified and eliminated from the data, it is posited that unreported subclinical seizures may persist, potentially influencing both the training and testing phases. Second, when the surgery was performed on this patient, the procedure resulted in Engle class II [53], which may have been caused by the incorrect identification of the original electrodes used in the simulations. A low number of samples to train the system can be another reason for poor performance for this patient. Pat-635, Pat-548, and Pat-818 also have an AUC lower than 0.8. The data for Pat-635 are collected from a 63-year-old woman whose epilepsy began when she was 30 years old. For this patient, the majority of reported seizures are related to the unclassified seizure category which may be the reason for the poor performance. More than 70% of reported seizures for Pat-548 and Pat-818 fall into the categories of simple partial and unclassified seizure types, which might negatively affect the system's effectiveness. Model-1 performs well for Pat-862 with the highest AUC of 1, lowest FPR of 0.01, and highest accuracy of 99.2%. The data are collected from a 16-year-old female experiencing seizures for four years. For this patient, no subclinical seizure is reported which can be one reason for having a good performance. Note that for this patient, 100% of seizures are the secondarily generalized seizures.

As shown in Tabel II, the mean method performs the best for the majority of patients, compared to other postprocessing methods. The worst performance is reported by Pat-139 with an AUC of .728. For this patient, 60% of the seizures are in the simple partial category which might be related to the poor

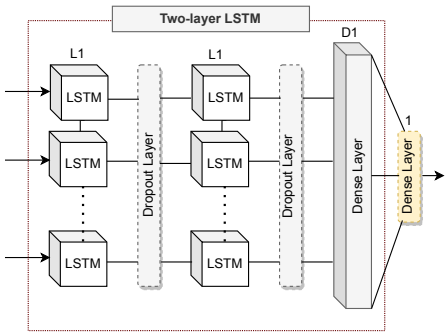

Details for each Model

Model	L1	D1	Num. of Parameters
Model 1	16	30	7,069
Model 2	32	50	20,901
Model 3	64	100	69,577
Model 4	128	100	237,257
Model 5	256	100	867,529

(b)

Fig. 7. (a) The structure of the classifier, which incorporates an LSTM model. (b) Details of each model used for evaluation.

TABLE I
EVALUATE THE EFFECT OF POST-PROCESSING METHOD ON THE RESULTS BASED ON MODEL-1

Model-1		*Sen* (%)			*FPR* (h^{-1})			*Acc* (%)			*AUC*		
Patient	Mean	MD	*kofn*	Mean	MD	*kofn*	Mean	MD	*kofn*	Mean	MD	*kofn*
Pat-970	81.52	82.7	78.7	0.23	0.22	0.20	77.8	78.4	80	0.87	0.87	0.79
Pat-1096	87.6	85.8	86.7	0.13	0.15	0.12	75.9	74.1	69.9	0.949	0.890	0.882
Pat-1084	86.1	77.3	84.2	0.19	0.19	0.16	82.0	80.3	83.5	0.94	0.89	0.84
Pat-958	88.3	91.7	83.3	0.12	0.16	0.10	87.8	84.8	89	0.926	0.928	0.864
Pat-922	92.5	90.8	90.0	0.23	0.21	0.22	80.7	81.8	81.2	0.927	0.918	0.825
Pat-273	72.2	60.8	69.9	0.28	0.28	0.24	72.1	71.6	75	0.863	0.808	0.708
Pat-253	100	100	97.2	0.38	0.44	0.29	65.7	59.6	73.3	0.76	0.753	0.663
Pat-862	100	100	95.9	0.01	0.03	0.01	99.2	97.2	98.8	1	0.975	0.975
Pat-620	100	100	100	0.29	0.25	0.27	74.7	72.7	76.3	0.98	0.995	0.87
Pat-1146	86.1	86.1	86.1	0.12	0.12	0.12	87.9	87.9	88.2	0.903	0.89	0.84
Pat-375	100	100	100	0.065	0.1	0.04	94.5	91.8	96.7	0.98	0.92	0.98
Pat-818	90.0	89.1	82.7	0.39	0.4	0.38	63.5	62.7	64.3	0.784	0.76	0.727
Pat-1073	91.5	89.8	79.5	0.32	0.27	0.28	70.5	74.5	72.7	0.846	0.842	0.758
Pat-916	80.6	75	80.6	0.12	0.22	0.11	87.3	77.8	88.1	0.91	0.793	0.847
Pat-635	72.2	75	66.7	0.24	0.3	0.19	76.1	70.7	79.2	0.767	0.793	0.703
Pat-565	94.4	94.4	94.4	0.21	0.2	0.19	81	82.1	82.6	0.95	0.94	0.86
Pat-264	100	100	95.85	0.32	0.36	0.32	70.7	68	71.1	0.84	0.895	0.82
Pat-1077	75.4	79.8	73.3	0.24	0.22	0.22	76.4	78.2	77.89	0.875	0.853	0.758
Pat-384	93.0	94.5	87.9	0.3	0.30	0.29	74.1	74.2	73.6	0.972	0.968	0.81
Pat-139	73.2	78.8	71.4	0.32	0.35	0.29	68.5	66.3	70.9	0.814	0.766	0.708
Pat-583	91.7	93.3	85	0.2	0.2	0.2	85.8	86.7	82.4	0.948	0.966	0.826
Pat-1125	86.1	91.7	86.1	0.35	0.34	0.34	67.4	68	70.1	0.813	0.798	0.758
Pat-548	66.7	66.7	65.7	0.37	0.34	0.35	64.9	66.4	65.1	0.764	0.792	0.652
Pat-590	71.7	70.5	70.6	0.02	0.02	0.01	84.6	83.9	84	0.981	0.966	0.841
Pat-115	75	72.9	75	0.18	0.11	0.19	80.3	85.7	79.9	0.813	0.818	0.783
Pat-442	72.8	70.5	70.6	0.16	0.16	0.12	83	82.3	85	0.828	0.841	0.785
Mean	**85.7**	**85.3**	**83**	**0.22**	**0.23**	**0.20**	**78.18**	**77.2**	**79.2**	**0.885**	**0.870**	**0.803**

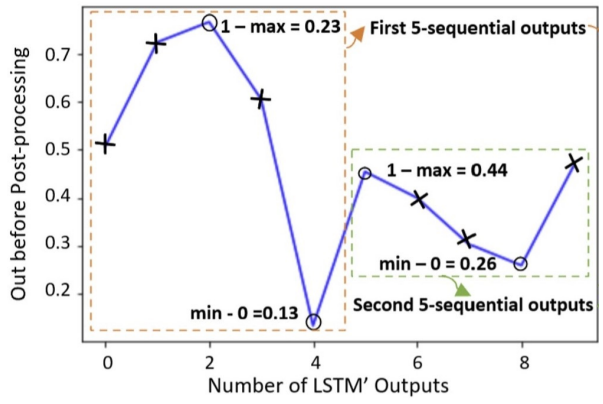

Fig. 8. An example of the MD Method.

performance. As the AUC decreases from 0.814 in Model 1 to 0.728 in Model 2, the low number of samples for training the system could be another reason. The reported AUC for Pat-590 is also among the highest reported AUC. This data is for an 18-year-old male who experienced a seizure when he was 11 years old. Several reasons might cause good performance. The patient's surgical outcome is classified as Engle class I, confirming that those electrodes used for simulation are correctly selected from the seizure onset zone. Further, all seizures are among the secondarily generalized and complex partial seizures. As displayed in Table III, the mean method in the post-processing achieves the best performance compared to other methods. The results for Pat-139 are still among the worst results compared to other patients. The reported results for Pat-862 are still among the best-reported results among all patients. Further, as shown in Tabel IV, the mean method still achieves the best performance.

As indicated in Table V, the best results are observed for Pat-862, with the highest accuracy and sensitivity both reaching 100%, the maximum AUC of 1, and the lowest FPR of zero. As mentioned before, there are no reported subclinical seizures for this patient, potentially contributing to the excellent performance. This underscores the influence of seizure type and

TABLE II
EVALUATE THE EFFECT OF POST-PROCESSING METHOD ON THE RESULTS BASED ON MODEL-2

Model-1		***Sen***	***(%)***		***FPR***	(h^{-1})		***Acc***	***(%)***		***AUC***	
Patient	**Mean**	**MD**	***kofn***	**Mean**	**MD**	***kofn***	**Mean**	**MD**	***kofn***	**Mean**	**MD**	***kofn***
Pat-970	80.0	80.5	79.5	0.31	0.29	0.28	70.6	72.1	73.2	0.85	0.84	0.76
Pat-1096	89.5	88.7	89.5	0.14	0.14	0.13	86.0	86.3	87	0.954	0.952	0.882
Pat-1084	79.1	77.3	77.4	0.2	0.21	0.18	80.3	79.2	81.8	0.94	0.916	0.768
Pat-958	86.7	85	85	0.16	0.17	0.14	84.5	83.4	85.6	0.89	0.89	0.852
Pat-922	92.5	89.2	90.8	0.25	0.24	0.23	79.9	79.6	80.5	0.916	0.874	0.838
Pat-273	60.8	65.3	60.8	0.35	0.32	0.31	65	67.4	68.6	0.818	0.818	0.65
Pat-253	94.5	94.4	94.5	0.32	0.32	0.3	70.2	70.45	72.5	0.9	0.847	0.823
Pat-862	87.5	87.5	87.5	0.02	0.02	0.01	97.6	97.6	98	0.995	0.98	0.935
Pat-620	100	100	100	0.2	0.23	0.19	82	79.6	83.6	0.975	0.985	0.91
Pat-1146	80.0	83.1	74	0.15	0.15	0.15	84.4	84.9	84.4	0.837	0.827	0.797
Pat-375	100	95.5	100	0.11	0.12	0.1	90.7	89	91.2	0.93	0.905	0.95
Pat-818	84.2	87.8	77.9	0.33	0.35	0.31	68.7	67.4	670	0.766	0.757	0.736
Pat-1073	79.38	81.1	70.9	0.26	0.27	0.20	75	73.7	79	0.836	0.818	0.75
Pat-916	75	86.1	75	0.09	0.16	0.06	90.1	84	91.9	0.91	0.863	0.833
Pat-635	64.1	55.8	61.3	0.36	0.30	0.33	66.2	70.5	68.3	0.84	0.723	0.75
Pat-565	94.4	91.7	94.4	0.14	0.12	.13	87.1	88.2	87.9	0.94	0.94	0.9
Pat-264	100	100	100	0.4	0.4	0.39	64.5	64.1	64.9	0.845	0.935	0.81
Pat-1077	80.1	84.3	77.9	0.2	0.23	0.22	76	77.5	78.1	0.908	0.905	0.78
Pat-384	94.5	94.5	92.9	0.28	0.27	0.27	75.7	76.6	76.3	0.97	0.954	0.828
Pat-139	64.1	71.4	64.1	0.32	0.35	0.30	68.0	65.6	69.5	0.728	0.686	0.696
Pat-583	91.7	96.7	80	0.25	0.22	0.25	83.2	87.4	77.3	0.944	0.928	0.84
Pat-1125	90.3	91.7	90.3	0.33	0.33	0.32	69	69.5	70	0.778	0.78	0.788
Pat-548	63.6	62.8	58.8	0.37	0.35	0.34	63.5	64.0	62.6	0.784	0.77	0.623
Pat-590	64.1	73.9	66.4	0	0.02	0	82	85.7	82	0.977	0.957	0.816
Pat-115	73	68.8	73	0.11	0.09	0.09	86.3	86.6	87.8	0.81	0.725	0.823
Pat-442	69.7	72.9	67.4	0.23	0.2	0.19	76.6	79.7	79.5	0.821	0.826	0.767
Mean	**82.3**	**83.3**	**80.4**	**0.23**	**0.23**	**0.21**	**77.8**	**78.1**	**78.9**	**0.88**	**0.862**	**0.804**

TABLE III
EVALUATE THE EFFECT OF POST-PROCESSING METHOD ON THE RESULTS BASED ON MODEL-3

Model-1		***Sen***	***(%)***		***FPR***	(h^{-1})		***Acc***	***(%)***		***AUC***	
Patient	**Mean**	**MD**	***kofn***	**Mean**	**MD**	***kofn***	**Mean**	**MD**	***kofn***	**Mean**	**MD**	***kofn***
Pat-970	77.7	76.6	76.6	0.25	0.23	0.22	75.0	76.6	77.6	0.86	0.84	0.77
Pat-1096	87.5	88.8	85.7	0.15	0.15	0.14	85.4	85.3	86.5	0.951	0.94	0.856
Pat-1084	80.9	70.0	79.2	0.2	0.2	0.19	80.1	79.4	80.6	0.896	0.91	0.8
Pat-958	83.3	90.0	80	0.13	0.16	0.12	87.0	84.2	86.9	0.912	0.892	0.84
Pat-922	92.5	89.2	90	0.23	0.22	0.21	80.9	81.1	82.2	0.912	0.881	0.845
Pat-273	60.6	60.4	51.7	0.24	0.26	0.23	75.4	68.5	70.8	0.838	0.783	0.65
Pat-253	100	97.2	100	0.45	0.49	0.38	59.0	55.5	65.4	0.9	0.803	0.807
Pat-862	95.9	95.9	95.9	0.02	0.04	0.02	98.4	96.4	98.4	0.99	0.97	0.97
Pat-620	100	100	100	0.22	0.25	0.2	80.4	78	82.4	0.99	0.995	0.9
Pat-1146	65.6	65.4	62.6	0.08	0.1	0.06	90	88	91.0	0.86	0.85	0.783
Pat-375	100	100	100	0.11	0.15	0.11	90.1	90.5	94.4	0.91	0.905	0.945
Pat-818	85.5	89.2	74.6	0.37	0.40	0.34	65.6	62.5	66.7	0.753	0.758	0.7
Pat-1073	88.0	87.9	81.2	0.28	0.28	0.25	73.4	73.4	75.7	0.842	0.816	0.782
Pat-916	91.7	83.3	91.7	0.24	0.26	0.21	77.7	75.4	79.7	0.88	0.817	0.85
Pat-635	66.7	66.7	63.9	0.3	0.28	0.28	70	71.5	71.8	0.8	0.753	0.68
Pat-565	94.4	88.9	88.9	0.14	0.12	0.13	86.5	88.2	87.0	0.94	0.93	0.88
Pat-264	91.7	91.7	91.7	0.4	0.44	0.4	63	59.4	63.3	0.775	0.82	0.76
Pat-1077	86.7	82.2	76	0.28	0.25	0.27	73.3	75.6	73.1	0.813	0.833	0.743
Pat-384	94.5	94.5	89.5	0.27	0.27	0.26	76.9	76.9	76.6	0.964	0.96	0.816
Pat-139	66.7	75.2	59.4	0.31	0.37	0.26	69.3	64.2	73	0.722	0.716	0.67
Pat-583	81.7	88.3	78.3	0.24	0.24	0.22	79.0	82.3	78.2	0.956	0.916	0.782
Pat-1125	88.2	91	88.2	0.36	0.36	0.35	66.7	66.6	67.3	0.815	0.763	0.765
Pat-548	60.9	59.1	58.8	0.37	0.33	0.32	62.0	63.3	63.5	0.737	0.728	0.633
Pat-590	64	66.3	59	0.02	0.05	0.02	80.1	80.7	78.2	0.953	0.943	0.784
Pat-115	73	70.9	70.8	0.08	0.06	0.08	88.3	89.1	87.4	0.805	0.83	0.813
Pat-442	64.4	62.5	63.4	0.16	0.18	0.14	82.1	80.6	83.9	0.821	0.83	0.75
Mean	**82.4**	**82**	**79.1**	**0.23**	**0.24**	**0.21**	**77.5**	**76.7**	**78.5**	**0.869**	**0.853**	**0.791**

data characteristics on the system's efficacy.

The impact of post-processing techniques, namely mean, MD, and K-of-N, on evaluation metrics (sensitivity, FPR, accuracy, and AUC) is summarized in Figure 9. Notably, the AUC values demonstrate that the mean method outperforms MD and K-of-N techniques across all models during post-processing. Consequently, the mean technique is adopted during the postprocessing stage.

B. Evaluation of the Effect of Model Complexity on the Results

As outlined in the preceding section, the mean method in post-processing demonstrated superior performance compared to MD and K-of-N methods. Consequently, to assess the impact of model complexity on system performance, the average outcomes for the mean method are compared across different models. The comparative results for each patient are shown in Figure 10. Notably, an increase in model size enhances results for certain patients, attributed to the complexity of their data, thereby indicating that a larger model yields improved outcomes. However, for some patients, enlarging the model

TABLE IV
EVALUATE THE EFFECT OF POST-PROCESSING METHOD ON THE RESULTS BASED ON MODEL-4

Model-1		*Sen*	*(%)*		*FPR*	*(h^{-1})*		*Acc*	*(%)*		*AUC*	
Patient	**Mean**	**MD**	***kofn***	**Mean**	**MD**	***kofn***	**Mean**	**MD**	***kofn***	**Mean**	**MD**	***kofn***
Pat-970	82.8	80.6	79.4	0.27	0.29	0.25	73.6	72.5	76.1	0.88	0.86	0.78
Pat-1096	91.3	89.7	89.5	0.17	0.17	0.16	83.6	84.08	84.6	0.949	0.942	0.869
Pat-1084	80.8	78.9	80.9	0.18	0.19	0.16	81.6	80.7	83.6	0.926	0.93	0.822
Pat-958	95.0	86.7	86.7	0.16	0.15	0.15	85.1	84.9	85.5	0.91	0.936	0.858
Pat-922	92.5	90.8	89.2	0.23	0.22	0.22	81.3	81.3	81.1	0.911	0.889	0.837
Pat-273	68.6	75.4	66.5	0.21	0.2	0.17	78	78.3	81.6	0.815	0.808	0.748
Pat-253	97.2	88.9	88.9	0.27	0.34	0.22	75.0	68.4	79.1	0.88	0.767	0.833
Pat-862	95.9	100	95.9	0.02	0.05	0.01	98.4	96	98.8	1	0.97	0.975
Pat-620	100	100	100	0.17	0.15	0.15	84.9	86.1	86.5	0.985	0.995	0.925
Pat-1146	83.3	80.3	77.5	0.11	0.09	0.09	89	90	89.7	0.873	0.84	0.843
Pat-375	100	100	100	0.1	0.15	0.1	91.6	87.3	91.2	0.95	0.94	0.93
Pat-818	86.3	87.6	85.01	0.36	0.37	0.34	66.5	65.7	68.1	0.793	0.784	0.757
Pat-1073	88.02	84.38	82.86	0.31	0.26	0.28	71.1	75.1	73.3	0.83	0.834	0.776
Pat-916	86.1	83.3	80.6	0.14	0.19	0.12	85.8	81.2	87.8	0.907	0.833	0.847
Pat-635	58.3	50	55.6	0.21	0.20	0.21	77.4	44.9	76.9	0.737	0.713	0.673
Pat-565	88.9	86.1	86.1	0.16	0.13	0.16	84	86.8	84.3	0.93	0.88	0.85
Pat-264	79.2	83.4	70.9	0.23	0.25	0.23	77.4	75.8	77	0.835	0.89	0.745
Pat-1077	93.6	87.1	89.2	0.3	0.3	0.26	72.6	71.3	75.5	0.878	0.795	0.8175
Pat-384	92.9	92.9	92.9	0.24	0.26	0.22	78.9	77.5	80.4	0.97	0.956	0.85
Pat-139	71.4	71.4	71.4	0.31	0.35	0.23	69.1	65.6	71.8	0.734	0.684	0.716
Pat-583	91.7	95	86.7	0.25	0.22	0.24	83.2	86.6	81.6	0.962	0.954	0.816
Pat-1125	86.1	82.7	86.1	0.32	0.32	0.31	69.5	69.2	70.9	0.79	0.75	0.778
Pat-548	57.3	59.5	56.3	0.34	0.35	0.33	61.8	62.4	61.9	0.758	0.727	0.616
Pat-590	62.8	71.4	60.3	0.05	0.09	0.05	78.9	81.3	77.6	0.95	0.961	0.776
Pat-115	75	75	75	0.21	0.18	0.16	78.2	81.1	82.4	0.83	0.823	0.798
Pat-442	70.7	68.7	69.6	0.19	0.16	0.16	80.4	82.5	82.8	0.791	0.809	0.77
Mean	**83.7**	**82.7**	**80.9**	**0.21**	**0.22**	**0.19**	**79.1**	**77.6**	**80.4**	**0.876**	**0.857**	**0.808**

TABLE V
EVALUATE THE EFFECT OF POST-PROCESSING METHOD ON THE RESULTS BASED ON MODEL-5

Model-1		*Sen*	*(%)*		*FPR*	*(h^{-1})*		*Acc*	*(%)*		*AUC*	
Patient	**Mean**	**MD**	***kofn***	**Mean**	**MD**	***kofn***	**Mean**	**MD**	***kofn***	**Mean**	**MD**	***kofn***
Pat-970	84.3	81.6	80.5	0.26	0.26	0.23	73.8	74.8	77.0	0.85	0.86	0.79
Pat-1096	84.6	88.5	81.8	0.15	0.15	0.14	84.7	85.7	85.9	0.934	0.948	0.841
Pat-1084	82.7	80.9	80.9	0.22	0.19	0.20	78.8	81.2	79.9	0.906	0.93	0.802
Pat-958	86.7	86.7	81.7	0.19	0.20	0.20	81.4	80.6	80.8	0.884	0.878	0.812
Pat-922	95	88.3	92.5	0.33	0.34	0.32	74	72.1	74.4	0.903	0.852	0.802
Pat-273	60.2	68.7	51.4	0.22	0.21	0.2	76.3	78.2	77.6	0.82	0.82	0.66
Pat-253	75	58.3	63.9	0.21	0.21	0.18	78.9	78.5	79.9	0.853	0.787	0.727
Pat-862	100	100	100	0	0	0	100	100	100	1	1	1
Pat-620	100	100	100	0.16	0.16	0.15	85.3	85.7	86.9	0.975	1	0.93
Pat-1146	77	77.0	77	0.12	0.13	0.12	86.9	86.6	87.4	0.873	0.857	0.827
Pat-375	100	100	100	0.06	0.17	0.05	95.1	85.7	95.6	0.965	0.865	0.975
Pat-818	86.4	86.2	83.9	0.35	0.36	0.33	67.4	69.5	68.5	0.811	0.793	0.754
Pat-1073	82.9	77.9	77.7	0.27	0.26	0.23	73.7	73.7	77	0.846	0.82	0.774
Pat-916	80.6	83.3	77.8	0.18	0.18	0.15	82.2	82.47	83.9	0.9	0.837	0.813
Pat-635	63.9	61.1	58.3	0.47	0.37	0.38	59.07	62.6	61.4	0.68	0.66	0.603
Pat-565	91.7	86.1	91.7	0.15	0.14	0.13	85.7	86.3	87.6	0.92	0.88	0.89
Pat-264	83.4	87.5	79.2	0.3	0.38	0.3	71.5	64.8	71.1	0.79	0.79	0.735
Pat-1077	80.5	78.4	78.4	0.16	0.18	0.13	84	81.8	85	0.91	0.883	0.825
Pat-384	94.5	92.9	94.5	0.24	0.25	0.24	79.5	59.1	79.5	0.966	0.972	0.852
Pat-139	75.3	75.3	75.3	0.35	0.42	0.33	65.6	59.6	68.2	0.76	0.754	0.714
Pat-583	100	100	96.7	0.2	0.2	0.2	90	90	88.34	0.966	0.93	0.9
Pat-1125	90.3	87.5	88.2	0.31	0.31	0.3	71.1	71.5	72.1	0.783	0.808	0.793
Pat-548	51.3	51.4	50.4	0.289	0.27	0.25	61.2	62.3	62.8	0.7167	0.68	0.627
Pat-590	63.8	67.5	57.5	0.02	0.04	0.013	80.67	82	78.2	0.947	0.929	0.781
Pat-115	60.4	68.8	60.4	0.08	0.13	0.07	85.3	83.7	86.2	0.708	0.8	0.77
Pat-442	64.4	60.3	63.4	0.15	0.15	0.13	83.1	82.4	86.6	0.776	0.778	0.751
Mean	**81.3**	**80.5**	**78.6**	**0.21**	**0.22**	**0.19**	**79.0**	**77.7**	**80**	**0.863**	**0.850**	**0.798**

diminishes performance, possibly due to overfitting, resulting in a consistent average performance as illustrated in Figure 11. Further, the figure indicates that augmenting the LSTM size does not markedly influence average results. Although a more complex model might be expected to yield better outcomes, simulation results revealed minimal changes, likely due to averaging results across 26 patients. While individual patient results may exhibit noticeable changes with increased model size, the overall average remains relatively constant. The comparative analysis further reveal that Model-1, employing the mean method in postprocessing, achieved the highest AUC compared to other model sizes.

C. Comparative Analysis with Prior Models

Table VII presents a comparative analysis between our proposed epilepsy prediction model and previous models. It is crucial to highlight that, unlike studies conducted on the Melbourne dataset, MIT dataset, American Society, and Bonn datasets that typically reported results for number of patients between 3 and up to 23, our results in this table are specifically for 26 epileptic seizure patients from the European dataset. The assessment of our model is based on four key metrics, namely sensitivity, FPR, accuracy, and AUC. In contrast to some systems that report only one or two metrics, our comprehensive evaluation provides a more robust understanding

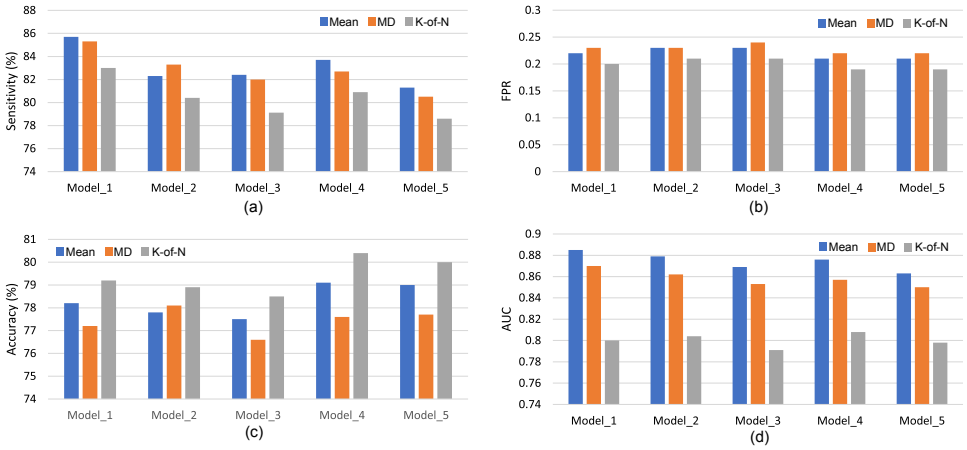

Fig. 9. A summary of the effect of various postprocessing techniques on the system's performance.

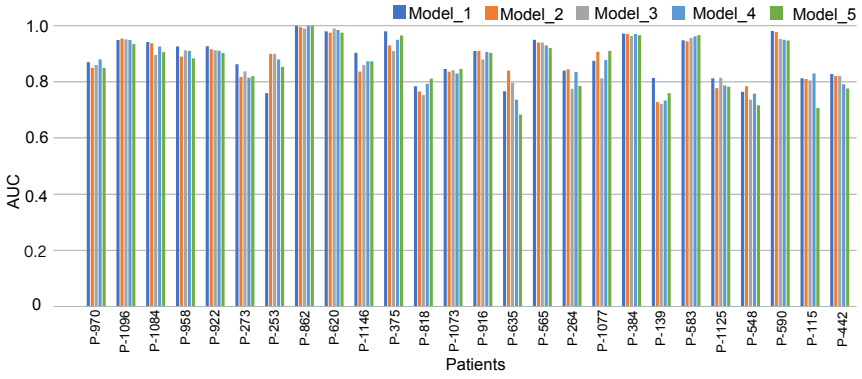

Fig. 10. The effect of model's complexity on the system's performance for each patient.

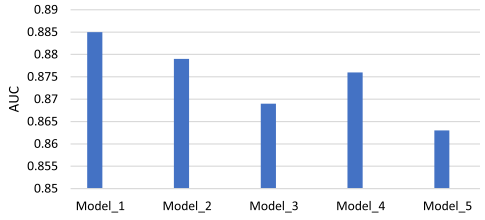

Fig. 11. The imapct of model's complexity on the AUC.

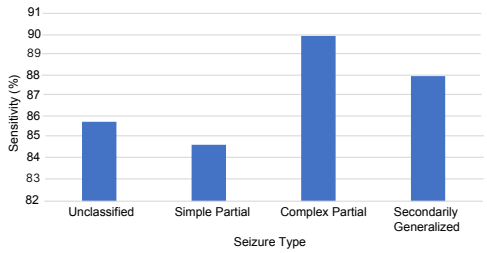

Fig. 12. The effect of various seizure types on the sensitivity.

of the system's performance. Note that this work marks the first instance of applying the iEEG European dataset, and our proposed model demonstrates commendable performance with low complexity. Importantly, we introduce an effective and simple model that utilizes only 4 electrodes, making it suitable for both implanted and wearable technology applications. This resulted in a classifier with fewer parameters—just 7,069—and a lower level of complexity. However, many reported models tend to be more complex, with a high number of trainable parameters. As an example, we note that the lists of trainable parameters for models in [24], [34], [32], and [33] are, respectively, 18,354, 20,125, 2,200,000, and 69,129,612, which clarifies the significant variation in complexity across the range of suggested approaches. Therefore, our proposed model strikes a balance between complexity and accuracy and thus has the potential to be implemented in resource-constrained devices, including wearables and implants.

D. The Effect of Seizure Types on the Prediction Performance

The types of seizures for each patient are included in the European iEEG dataset. Based on the seizure classifications [54], every seizure in this dataset is categorized as either complex partial (CP), secondarily generalized (SG), simple partial (SP), or unclassified (U). It is worth mentioning that secondarily generalized seizures and partial seizures are replaced by bilateral tonic-clonic seizures and focal seizures, respectively by the ILAE from 1981 classification in 2017 [54]. In this section, we investigate the impact of the seizure type on the prediction results. In Table VI, the AUC and sensitivity for

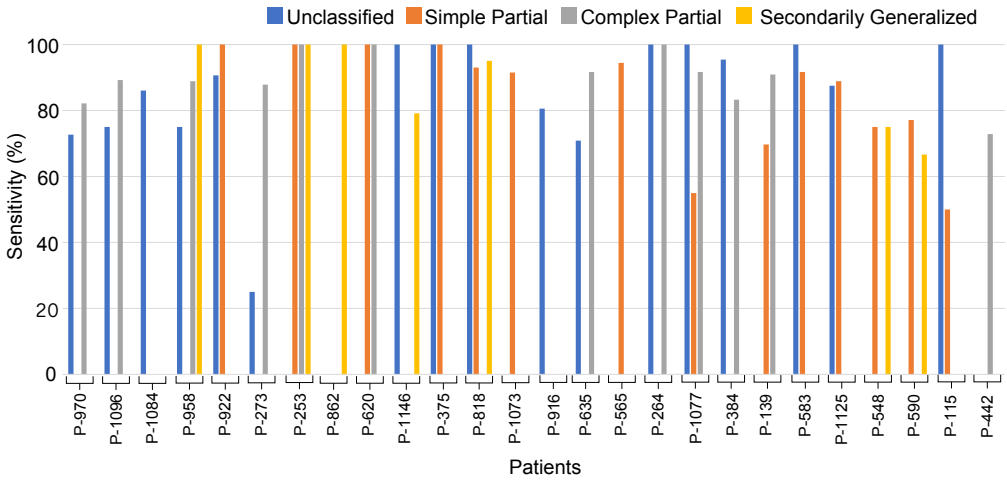

Fig. 13. The effect of seizure type on model's sensitivity for each patient.

TABLE VI
SYSTME'S PERFORMANCE AND THE PERCENTAGE OF SEIZURE TYPES USED FOR EACH PATIENT IN THE IEEG EUROPEAN DATASET.

Model-1 Patient	*Sen(%)* (%)	*AUC*	*SG* (%)	*CP* (%)	*SP* (%)	*U* (%)
Pat-970	81.52	0.87	0	93.3	0	6.7
Pat-1096	87.6	0.949	0	88.9	0	11.1
Pat-1084	86.1	0.94	0	0	0	100
Pat-958	88.3	0.926	20	60	0	20
Pat-922	92.5	0.927	0	0	20	80
Pat-273	72.2	0.863	0	75	0	25
Pat-253	100	0.76	33.3	33.3	33.3	0
Pat-862	100	1	100	0	0	0
Pat-620	100	0.98	0	50	50	0
Pat-1146	86.1	0.903	0	66.7	0	33.3
Pat-375	100	0.98	0	0	50	50
Pat-818	90.0	0.784	28.6	0	57.1	14.3
Pat-1073	91.5	0.846	0	0	100	0
Pat-916	80.6	0.91	0	0	0	100
Pat-635	72.2	0.767	0	33.3	0	66.7
Pat-565	94.4	0.95	0	0	100	0
Pat-264	100	0.84	0	50	0	50
Pat-1077	75.4	0.875	0	25	50	25
Pat-384	93.0	0.972	0	20	0	80
Pat-139	73.2	0.814	0	40	60	0
Pat-583	91.7	0.948	0	0	80	20
Pat-1125	86.1	0.813	0	0	50	50
Pat-548	66.7	0.764	11.1	0	88.9	0
Pat-590	71.7	0.981	28.6	71.4	0	0
Pat-115	75	0.813	0	0	50	50
Pat-442	72.8	0.828	0	100	0	0

model-1 using the mean method in the postprocessing stage are presented for each patient. The last four columns on the right side indicate the percentage of each seizure type present in the data for each patient in the simulation. For example, Pat-970 does not experience SG or U seizures, while 93.3% and 6.70% are CP and SP seizures, respectively.

In the following results, sensitivity is used as the primary metric to evaluate the system's effectiveness, as seizure type can significantly impact the sensitivity measure. The average sensitivity for each patient based on seizure type is represented in Figure 13. As indicated in the figure, the seizure type affects the sensitivity, where the lowest reported sensitivity is related to the unclassified seizure type for Pat-273, while the complex partial type has a sensitivity of 87.87%. Furthermore, the reported sensitivity of unclassified and simple partial categories for each patient is often lower than the reported sensitivity of complex partial and secondary generalized seizure types. Moreover, the lowest sensitivity of SG, CP, SP, and U are 66.65%, 72.83%, 50%, and 25%, respectively. This confirms that the epileptic prediction system can have better performance on those patients with CP and SG seizures compared to those patients suffering from SP and U seizures. The average sensitivity for each seizure category is shown in Figure 12. The average results indicate that CP seizures have the highest sensitivity of 89.9% while the lowest sensitivity is related to SP seizures. Thus, the seizure types can explain the reasons behind the system's good or poor performance for each patient.

V. DISCUSSION AND FUTURE WORK

In this study, we have presented a model that stands out for its good performance and low complexity. We achieved this by selectively using four electrodes to simplify the model architecture. This resulted in a classifier with fewer parameters—just 7,069—and a lower level of complexity. Twenty-six patients were used in our simulation framework. However, including more patients can lead to more substantial and impactful results. Future work aims to expand upon these findings by incorporating a larger patient sample size. Note that our findings highlight how important it is to have accurate information about the origin electrodes, seizure onset zones, and electrode placement of each patient during the electrode selection step. Consequently, databases utilized for this purpose must comprehensively obtain these pertinent details. As a result, the use of some publicly accessible datasets like the Melbourne Dataset and the American Epilepsy Society Dataset may be limited since they do not contain these essential details.

Our proposed model operates on a patient-specific basis, requiring tailored retraining and testing procedures for each individual. Looking ahead, we aspire to refine our model to achieve patient-independent, streamlining processes for broader applicability and efficiency. Generally, there is a trade-off between complexity and performance. Maintaining a balance between these factors will be essential as we work to improve our model's efficacy and complexity. Since we aimed to present a model with lower complexity, our model's performance has to be enhanced by decreasing FPR. Using CNNs for feature extraction instead of hand-crafted features is one way to make improvements. However, it's crucial to

TABLE VII
REPORTED RESULTS ON EPILEPSY PREDICTION ALGORITHMS

Ref.	dataset	*Preprocessing*	*Feature Extraction*	*Classification*	*Post-processing*	*Sensitivity %*	*FPR %*	*Accuracy %*	*AUC*
[31]	Melbourne	Down-sampling	STFT	CNN	-	87.85	-	-	
[32]	Melbourne CHB-MIT	Notch Filter	STFT	Convolutional Epileptic Network(CESP)	-	78.11 88.21	0.14 0.27	-	
[33]	Melbourne CHB-MIT	Continuous Wavelet Transform (CWT)	-	Semi-dilated Convolution Convolution Network(SDCN)	-	88.45 98.9	- -	- -	0.883 .928
[8]	Melbourne	-	EEG Scalogram	Multi-Channel Vision Transform (MViT)	-	91.15	-	-	0.924
[55]	Melbourne	-	-	CNN	-	85.2-86.3	-	-	0.914- 0.933
[56]	Melbourne	-	-	MLP	-	-	-	-	0.815
[57]	Melbourne	-	Time and Frequency	Random Forest, Adaptive	-	-	-	-	0.844
[58]	Melbourne	-	Signal energy	Decision tree, kNN	-	33.67	-	-	-
[59]	Melbourne	-	Signal energy, Circadian profile	Logistic regression	-	52.67	-	-	-
[60]	Melbourne	-	EEG Spectrogram, Circadian profile	CNN	-	77.36	-	-	-
[34]	Melbourne	Filtering	Statistical Features in Time Domain, power in different frequency bands	Two-layer LSTM	K-of-N, MD, Mean	86.8	.147	85.1	92
[25]	American Epilepsy Society	-	STFT	CNN	K-of-N method	75	.21	-	
[26]	CHB-MIT	-	Time/Frequency Domain, Wavelet Transform, Cross Correlation, Graph Theory	2-layer LSTM	-	99.28-99.84	.02-.11	-	-
[24]	CHB-MIT	-	Deep Convolutional Autoencoder	BiLSTM	-	99.72	.004	99.66	-
[40]	CHB-MIT	-	STFT + CNN	LSTM	K-of-N method	98.21	.13	-	-
[29]	CHB-MIT	Filtering	Combination of Common Spatial Statistics	CNN	Kalman Filtering	92.2	.12	90	-
[28]	CHB-MIT	-	STFT	CRGNN	-	89	-	75.6	
[61]	CHB-MIT	-	Spectral power	SVM		98.7	0.04	-	-
[62]	CHB-MIT	-	Phase locking value	SVM		82.4	-	-	-
[63]	CHB-MIT	-	Mel-frequency spectral coefficient	Siamese NN		92.5	-	91.5	-
[64]	CHB-MIT	-	-	CNN		92	.136	-	-
[65]	CHB-MIT	-	Spectral-temporal feature	Graph convolution Network		95.5	0.109	-	-
[66]	CHB-MIT	-	EEG Spectrogram	LSTM		93	-	-	-
[67]	CHB-MIT	-	EEG Spectrogram	Residual network		89.3	-	92.1	-
[68]	CHB-MIT	-	Mel frequency Spectral coefficients	GNN		94.5	-	95.4	-
[69]	CHB-MIT	-	-	Diated CNN		93.3	0.007	-	-
[70]	CHB-MIT	-	- Spectrogram	ViT		59.2-97	-	-	-
[41]	Bonn	-	-	Stacked BiLSTM	-	89.21	.06	91	
Proposed model	European	CAR based Method	Time and Frequency	Two-layer LSTM	Mean	85.7	.22	78.1	0.885

acknowledge that such advancements may come at the expense of increased complexity. In this research, we also looked at how different seizure types affected the results. However, it is important to recognize that seizure type is just one aspect of a more complex picture. Incorporating a wider range of patient characteristics and illness background variables, such as age, gender, and seizure onset zone, among others, is crucial for thorough and detailed comparisons. We anticipate that these parameters will be incorporated into our studies in the future, which will enhance the scope and depth of our results.

VI. CONCLUSION

We proposed an epileptic seizure prediction system based on a two-layer LSTM and have conducted a detailed study, which is the first to utilize the large iEEG European dataset and analyze the impact of seizure type. We analyzed the results of five different model sizes and three different post-processing methods on a large set of patients. Simulation results indicate that the model with its simplest structure in conjunction with the mean method for postprocessing achieves the best performance, with an average AUC of 0.885. The system performance is comparable to the best of prior work despite its small model size. The results also show that the system performance is impacted by the seizure type. Specifically, the model performs better for individuals with *SG* and *CP* seizures compared to those with *SP* and *U* seizures. These findings may offer a new perspective for professionals working with individuals experiencing different seizure types.epileptic seizures.

VII. REFERENCES

[1] Z. Shi, Z. Liao, and H. Tabata, "Enhancing performance of convolutional neural network-based epileptic electroencephalogram diagnosis by asymmetric stochastic resonance," *IEEE Journal of Biomedical and Health Informatics*, vol. 27, no. 9, pp. 4228–4239, 2023.

[2] *https://www.who.int/news-room/fact-sheets/detail/epilepsy*. World Health Organization, 2018.

[3] D. Angeles *et al.*, "Proposal for revised clinical and electroencephalographic classification of epileptic seizures," *Epilepsia*, vol. 22, no. 4, pp. 489–501, 1981.

[4] J. J. Falco-Walter, I. E. Scheffer, and R. S. Fisher, "The new definition and classification of seizures and epilepsy," *Epilepsy research*, vol. 139, pp. 73–79, 2018.

[5] J. A. French, "Refractory epilepsy: clinical overview," *Epilepsia*, vol. 48, pp. 3–7, 2007.

[6] J. F. Téllez-Zenteno, L. H. Ronquillo, F. Moien-Afshari, and S. Wiebe, "Surgical outcomes in lesional and non-lesional epilepsy: a systematic review and meta-analysis," *Epilepsy research*, vol. 89, no. 2-3, pp. 310–318, 2010.

[7] I. Ahmad, X. Wang, D. Javeed, P. Kumar, O. W. Samuel, and S. Chen, "A hybrid deep learning approach for epileptic seizure detection in EEG signals," *IEEE Journal of Biomedical and Health Informatics*, pp. 1–12, 2023.

[8] R. Hussein, S. Lee, and R. Ward, "Multi-channel vision transformer for epileptic seizure prediction," *Biomedicines*, vol. 10, no. 7, p. 1551, 2022.

[9] V. Srinivasan, C. Eswaran, and N. Sriraam, "Approximate entropy-based epileptic EEG detection using artificial neural networks," *IEEE Transactions on information Technology in Biomedicine*, vol. 11, no. 3, pp. 288–295, 2007.

[10] M. Mula and F. Monaco, "Ictal and peri-ictal psychopathology," *Behavioural Neurology*, vol. 24, pp. 21–25, 2011.

[11] R. Brenner, F. Drislane, J. Ebersole, M. Grigg-Damberger, M. Hallett, S. Herman, L. Hirsch, A. Husain, P. Kaplan, A. Legatt, D. Nordli, G. Parry, M. Ross, D. Schomer, E. So, A. Sumner, and W. Tatum IV, "Guideline twelve: Guidelines for long-term monitoring for epilepsy," *The Neurodiagnostic journal*, vol. 48, pp. 265–286, Dec. 2008.

[12] V. Roy and S. Shukla, "Designing efficient blind source separation methods for EEG motion artifact removal based on statistical evaluation," *Wireless Personal Communications*, vol. 108, pp. 1311–1327, Oct 2019.

[13] X. Jiang, G.-B. Bian, and Z. Tian, "Removal of artifacts from EEG signals: A review," *Sensors (Basel, Switzerland)*, vol. 19, p. 987, Feb 2019.

[14] I. Daubechies, "The wavelet transform, time-frequency localization and signal analysis," *IEEE Transactions on Information Theory*, vol. 36, no. 5, pp. 961–1005, 1990.

[15] P. Flandrin, P. Gonçalvès, and G. Rilling, "Detrending and denoising with empirical mode decompositions," in *Proceedings of the 2004 12th European Signal Processing Conference*, pp. 1581–1584, 2004.

[16] R. R. Sreekrishna, S. Nalband, and A. A. Prince, "Real time cascaded moving average filter for detrending of electroencephalogram signals," in *Proceedings of the 2016 International Conference on Communication and Signal Processing (ICCSP)*, pp. 0745–0750, 2016.

[17] K. T. Sweeney, H. Ayaz, T. E. Ward, M. Izzetoglu, S. F. McLoone, and B. Onaral, "A methodology for validating artifact removal techniques for physiological signals," *IEEE transactions on information technology in biomedicine*, vol. 16, no. 5, pp. 918–926, 2012.

[18] R. G. Andrzejak, K. Lehnertz, F. Mormann, C. Rieke, P. David, and C. E. Elger, "Indications of nonlinear deterministic and finite-dimensional structures in time series of brain electrical activity: Dependence on recording region and brain state," *Phys. Rev. E*, vol. 64, p. 061907, Nov 2001.

[19] I. McNulty, S. M. Varnosfaderani, O. Makke, N. J. Sarhan, E. Asano, A. Luat, and M. Alhawari, "Analysis of artifacts removal techniques in EEG signals for energy-constrained devices," in *2021 IEEE International Midwest Symposium on Circuits and Systems (MWSCAS)*, pp. 515–519, IEEE, 2021.

[20] S. M. Varnosfaderani, I. McNulty, N. J. Sarhan, and M. Alhawari, "Artifacts removal techniques for the European iEEG dataset," in *2023 IEEE International Midwest Symposium on Circuits and Systems (MWSCAS)*.

[21] G. Li, S. Jiang, S. E. Paraskevopoulou, M. Wang, Y. Xu, Z. Wu, L. Chen, D. Zhang, and G. Schalk, "Optimal referencing for stereo-electroencephalographic (SEEG) recordings," *NeuroImage*, vol. 183, pp. 327–335, 2018.

[22] Y. Huang, B. Hajnal, L. Entz, D. Fabó, J. L. Herrero, A. D. Mehta, and C. J. Keller, "Intracortical dynamics underlying repetitive stimulation predicts changes in network connectivity," *Journal of Neuroscience*, vol. 39, no. 31, pp. 6122–6135, 2019.

[23] Y. Huang and C. Keller, "How can I investigate causal brain networks with iEEG?," *arXiv preprint arXiv:2205.07045*, 2022.

[24] H. Daoud and M. A. Bayoumi, "Efficient epileptic seizure prediction based on deep learning," *IEEE Transactions on Biomedical Circuits and Systems*, vol. 13, no. 5, pp. 804–813, 2019.

[25] N. D. Truong, A. D. Nguyen, L. Kuhlmann, M. R. Bonyadi, J. Yang, and O. Kavehei, "A generalised seizure prediction with convolutional neural networks for intracranial and scalp electroencephalogram data analysis," *CoRR*, vol. abs/1707.01976, 2017.

[26] kostas . Tsiouris, V. C. Pezoulas, M. Zervakis, S. Konitsiotis, D. D. Koutsouris, and D. I. Fotiadis, "A long short-term memory deep learning network for the prediction of epileptic seizures using EEG signals," *Computers in Biology and Medicine*, vol. 99, pp. 24 – 37, 2018.

[27] D. Thara, B. PremaSudha, and F. Xiong, "Epileptic seizure detection and prediction using stacked bidirectional long short term memory," *Pattern Recognition Letters*, vol. 128, pp. 529–535, 2019.

[28] A. Affes, A. Mdhaffar, C. Triki, M. Jmaiel, and B. Freisleben, "A convolutional gated recurrent neural network for epileptic seizure prediction," in *How AI Impacts Urban Living and Public Health* (J. Pagán, M. Mokhtari, H. Aloulou, B. Abdulrazak, and M. F. Cabrera, eds.), (Cham), pp. 85–96, Springer International Publishing, 2019.

[29] Y. Zhang, Y. Guo, P. Yang, W. Chen, and B. Lo, "Epilepsy seizure prediction on EEG using common spatial pattern and convolutional neural network," *IEEE Journal of Biomedical and Health Informatics*, vol. 24, no. 2, pp. 465–474, 2020.

[30] H. Khan, L. Marcuse, M. Fields, K. Swann, and B. Yener, "Focal onset seizure prediction using convolutional networks," *IEEE Transactions on Biomedical Engineering*, vol. 65, no. 9, pp. 2109–2118, 2017.

[31] R. Hussein, M. O. Ahmed, R. Ward, Z. J. Wang, L. Kuhlmann, and Y. Guo, "Human intracranial EEG quantitative analysis and automatic feature learning for epileptic seizure prediction," 2019.

[32] K. Rasheed, J. Qadir, T. J. O'Brien, L. Kuhlmann, and A. Razi, "A generative model to synthesize EEG data for epileptic seizure prediction," *IEEE Transactions on Neural Systems and Rehabilitation Engineering*, vol. 29, pp. 2322–2332, 2021.

[33] R. Hussein, S. Lee, R. Ward, and M. J. McKeown, "Epileptic seizure prediction: A semi-dilated convolutional neural network architecture," in *2020 25th International Conference on Pattern Recognition (ICPR)*, pp. 5436–5443, IEEE, 2021.

[34] S. M. Varnosfaderani, R. Rahman, N. J. Sarhan, L. Kuhlmann, E. Asano, A. Luat, and M. Alhawari, "A two-layer LSTM deep learning model for epileptic seizure prediction," in *2021 IEEE 3rd International Conference on Artificial Intelligence Circuits and Systems (AICAS)*, pp. 1–4, 2021.

[35] S. Gibson, J. W. Judy, and D. Markovic, "Technology-aware algorithm design for neural spike detection, feature extraction, and dimensionality reduction," *IEEE Transactions on Neural Systems and Rehabilitation Engineering*, vol. 18, no. 5, pp. 469–478, 2010.

[36] F. Ali, S. El-Sappagh, S. R. Islam, D. Kwak, A. Ali, M. Imran, and K.-S. Kwak, "A smart healthcare monitoring system for heart disease prediction based on ensemble deep learning and feature fusion," *Information Fusion*, vol. 63, pp. 208 – 222, 2020.

[37] I. Assali, A. G. Blaiech, A. B. Abdallah, K. B. Khalifa, M. Carrère, and M. H. Bedoui, "CNN-based classification of epileptic states for seizure prediction using combined temporal and spectral features," *Biomedical Signal Processing and Control*, vol. 82, p. 104519, 2023.

[38] Y. Ma, Z. Huang, J. Su, H. Shi, D. Wang, S. Jia, and W. Li, "A multi-channel feature fusion CNN-BI-LSTM epilepsy EEG classification and prediction model based on attention mechanism," *IEEE Access*, 2023.

[39] X. Lu, A. Wen, L. Sun, H. Wang, Y. Guo, and Y. Ren, "An epileptic seizure prediction method based on CBAM-3D CNN-LSTM model," *IEEE Journal of Translational Engineering in Health and Medicine*, 2023.

[40] M. Shahbazi and H. Aghajan, "A generalizable model for seizure prediction based on deep learning using CNN-LSTM architecture," in *Proceedings of the 2018 IEEE Global Conference on Signal and Information Processing (GlobalSIP)*, pp. 469–473, 2018.

[41] T. D.K., P. B.G., and F. Xiong, "Epileptic seizure detection and prediction using stacked bidirectional long short term memory," *Pattern Recognition Letters*, vol. 128, pp. 529 – 535, 2019.

[42] N. D. Truong, A. D. Nguyen, L. Kuhlmann, M. R. Bonyadi, J. Yang, S. Ippolito, and O. Kavehei, "Convolutional neural networks for seizure prediction using intracranial and scalp electroencephalogram," *Neural Networks*, vol. 105, pp. 104–111, 2018.

[43] G. Wang, D. Wang, C. Du, K. Li, J. Zhang, Z. Liu, Y. Tao, M. Wang, Z. Cao, and X. Yan, "Seizure prediction using directed transfer function and convolution neural network on intracranial EEG," *IEEE Transactions on Neural Systems and Rehabilitation Engineering*, vol. 28, no. 12, pp. 2711–2720, 2020.

[44] S. M. Varnosfaderani, R. Rahman, N. J. Sarhan, and M. Alhawari, "A self-aware power management model for epileptic seizure systems based on patient-specific daily seizure pattern," in *2023 International Conference on Microelectronics (ICM)*, pp. 91–95, IEEE, 2023.

[45] A. Shoeb, *Application of machine learning to epileptic seizure onset detection and treatment*. PhD thesis, 2009.

[46] "CHB-mit scalp EEG database, Physionet.org, [online]. available:https://physionet.org/content/chbmit/1.0.0/,."

[47] X. Ma, S. Qiu, Y. Zhang, X. Lian, and H. He, "Predicting epileptic seizures from intracranial EEG using LSTM-based multi-task learning," in *Chinese Conference on Pattern Recognition and Computer Vision (PRCV)*, pp. 157–167, Springer, 2018.

[48] N. V. Chawla, N. Japkowicz, and A. Kotcz, "Special issue on learning from imbalanced data sets," *ACM SIGKDD explorations newsletter*, vol. 6, no. 1, pp. 1–6, 2004.

[49] *European Epilepsy Dataset*. EPILEPSIAE project, 2020. http://epilepsy-database.eu/.

[50] R. Rahman, S. M. Varnosfaderani, O. Makke, N. J. Sarhan, E. Asano, A. Luat, and M. Alhawari, "Comprehensive analysis of EEG datasets for epileptic seizure prediction," in *2021 IEEE International Symposium on Circuits and Systems (ISCAS)*, pp. 1–5, IEEE, 2021.

[51] F. Bao, X. Liu, and C. Zhang, "PyEEG: An open source python module for EEG/MEG feature extraction," in *Computational Intelligence and Neuroscience*, 2011.

[52] L. Prechelt, "Early stopping-but when?," in *Neural Networks: Tricks of the trade*, pp. 55–69, Springer, 2002.

[53] S. West, S. J. Nevitt, J. Cotton, S. Gandhi, J. Weston, A. Sudan, R. Ramirez, and R. Newton, "Surgery for epilepsy," *Cochrane Database of Systematic Reviews*, no. 6, 2019.

[54] R. S. Fisher, J. H. Cross, J. A. French, N. Higurashi, E. Hirsch, F. E. Jansen, L. Lagae, S. L. Moshé, J. Peltola, E. Roulet Perez, *et al.*, "Operational classification of seizure types by the international league against epilepsy: Position paper of the ILAE commission for classification and terminology," *Epilepsia*, vol. 58, no. 4, pp. 522–530, 2017.

[55] S. Zhao, J. Yang, and M. Sawan, "Energy-efficient neural network for epileptic seizure prediction," *IEEE Transactions on Biomedical Engineering*, vol. 69, no. 1, pp. 401–411, 2021.

[56] C. Reuben, P. Karoly, D. R. Freestone, A. Temko, A. Barachant, F. Li, G. Titericz Jr, B. W. Lang, D. Lavery, K. Roman, *et al.*, "Ensembling crowdsourced seizure prediction algorithms using long-term human intracranial EEG," *Epilepsia*, vol. 61, no. 2, pp. e7–e12, 2020.

[57] L. Kuhlmann, P. Karoly, D. R. Freestone, B. H. Brinkmann, A. Temko, A. Barachant, F. Li, G. Titericz Jr., B. W. Lang, D. Lavery, K. Roman, D. Broadhead, S. Dobson, G. Jones, Q. Tang, I. Ivanenko, O. Panichev, T. Proix, M. NÃ¡hlÃk, D. B. Grunberg, C. Reuben, G. Worrell, B. Litt, D. T. J. Liley, D. B. Grayden, and M. J. Cook, "Epilepsyecosystem.org: crowd-sourcing reproducible seizure prediction with long-term human intracranial EEG," *Brain: a journal of neurology*, vol. 141, pp. 2619–2630, Sep 2018. 30101347 [pmid].

[58] M. J. Cook, T. J. O'Brien, S. F. Berkovic, M. Murphy, A. Morokoff, G. Fabinyi, W. D'Souza, R. Yerra, J. Archer, L. Litewka, *et al.*, "Prediction of seizure likelihood with a long-term, implanted seizure advisory system in patients with drug-resistant epilepsy: a first-in-man study," *The Lancet Neurology*, vol. 12, no. 6, pp. 563–571, 2013.

[59] P. J. Karoly, H. Ung, D. B. Grayden, L. Kuhlmann, K. Leyde, M. J. Cook, and D. R. Freestone, "The circadian profile of epilepsy improves seizure forecasting," *Brain*, vol. 140, no. 8, pp. 2169–2182, 2017.

[60] I. Kiral-Kornek, S. Roy, E. Nurse, B. Mashford, P. Karoly, T. Carroll, D. Payne, S. Saha, S. Baldassano, T. O'Brien, *et al.*, "Epileptic seizure prediction using big data and deep learning: toward a mobile system," *EBioMedicine*, vol. 27, pp. 103–111, 2018.

[61] Z. Zhang and K. K. Parhi, "Low-complexity seizure prediction from iEEG/sEEG using spectral power and ratios of spectral power," *IEEE transactions on biomedical circuits and systems*, vol. 10, no. 3, pp. 693–706, 2015.

[62] D. Cho, B. Min, J. Kim, and B. Lee, "EEG-based prediction of epileptic seizures using phase synchronization elicited from noise-assisted multivariate empirical mode decomposition," *IEEE Transactions on Neural Systems and Rehabilitation Engineering*, vol. 25, no. 8, pp. 1309–1318, 2016.

[63] T. Dissanayake, T. Fernando, S. Denman, S. Sridharan, and C. Fookes, "Deep learning for patient-independent epileptic seizure prediction using scalp EEG signals," *IEEE Sensors Journal*, vol. 21, no. 7, pp. 9377–9388, 2021.

[64] R. Jana and I. Mukherjee, "Deep learning based efficient epileptic seizure prediction with EEG channel optimization," *Biomedical Signal Processing and Control*, vol. 68, p. 102767, 2021.

[65] Y. Li, Y. Liu, Y.-Z. Guo, X.-F. Liao, B. Hu, and T. Yu, "Spatio-temporal-spectral hierarchical graph convolutional network with semisupervised active learning for patient-specific seizure prediction," *IEEE transactions on cybernetics*, vol. 52, no. 11, pp. 12189–12204, 2021.

[66] S. M. Usman, S. Khalid, and Z. Bashir, "Epileptic seizure prediction using scalp electroencephalogram signals," *Biocybernetics and Biomedical Engineering*, vol. 41, no. 1, pp. 211–220, 2021.

[67] X. Yang, J. Zhao, Q. Sun, J. Lu, and X. Ma, "An effective dual self-attention residual network for seizure prediction," *IEEE Transactions on Neural Systems and Rehabilitation Engineering*, vol. 29, pp. 1604–1613, 2021.

[68] T. Dissanayake, T. Fernando, S. Denman, S. Sridharan, and C. Fookes, "Geometric deep learning for subject independent epileptic seizure prediction using scalp EEG signals," *IEEE Journal of Biomedical and Health Informatics*, vol. 26, no. 2, pp. 527–538, 2021.

[69] Y. Gao, X. Chen, A. Liu, D. Liang, L. Wu, R. Qian, H. Xie, and Y. Zhang, "Pediatric seizure prediction in scalp EEG using a multi-scale neural network with dilated convolutions," *IEEE journal of translational engineering in health and medicine*, vol. 10, pp. 1–9, 2022.

[70] X. Zhang and H. Li, "Patient-specific seizure prediction from scalp EEG using vision transformer," in *2022 IEEE 6th Information Technology and Mechatronics Engineering Conference (ITOEC)*, vol. 6, pp. 1663–1667, IEEE, 2022.